

MetaTra: Meta-Learning for Generalized Trajectory Prediction in Unseen Domain

Abstract

Trajectory prediction has garnered widespread attention in different fields, such as autonomous driving and robotic navigation. However, due to the significant variations in trajectory patterns across different scenarios, models trained in known environments often falter in unseen ones. To learn a generalized model that can directly handle unseen domains without requiring any model updating, we propose a novel meta-learning-based trajectory prediction method called *MetaTra*. This approach incorporates a *Dual Trajectory Transformer (Dual-TT)*, which enables a thorough exploration of the individual intention and the interactions within group motion patterns in diverse scenarios. Building on this, we propose a meta-learning framework to simulate the generalization process between source and target domains. Furthermore, to enhance the stability of our prediction outcomes, we propose a *Serial and Parallel Training (SPT)* strategy along with a feature augmentation method named *MetaMix*. Experimental results on several real-world datasets confirm that *MetaTra* not only surpasses other state-of-the-art methods but also exhibits plug-and-play capabilities, particularly in the realm of domain generalization. [16] [27] [38] [1]

1. Introduction

Trajectory prediction plays a pivotal role in domains like robotic navigation, security surveillance, and sports analytics. Particularly with the rapid advancements of the autonomous driving industry, accurately predicting the trajectories of transportation elements is a key factor that influences the decision-making process of autonomous vehicles [12, 47, 50, 51]. Initially reliant on physics-based techniques, such as the Kalman filter [35] and Monte Carlo methods [9], the field of trajectory prediction has now shifted towards the adoption of machine learning approaches [8, 12, 17]. Further advancements have been realized with the integration of reinforcement learning frameworks, including MDP [7] and GAIL [18], as well as advanced deep learning algorithms like LSTM [2] and Transformer [45]. These developments have notably improved the accuracy in predicting track sequences. Simultaneously, the compatibility of graphs with Non-Euclidean data facilitates the effective modeling of complex interactions, prompting researchers to

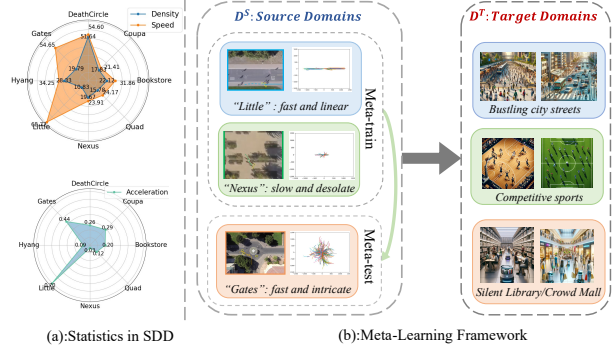


Figure 1. In part (a), we quantify the statistical biases in various scenarios within the SDD. The terms “Density”, “Speed”, and “Acceleration” refer to the average pedestrian count, velocity, and acceleration metrics for each sequence, respectively. In part (b), our approach to the generalized trajectory prediction challenge is presented. It shows three source domains on the left for training, each with distinct trajectory distributions, and some unfamiliar target domains on the right for testing. Our model acquires domain-invariant universal knowledge by simulating domain shifts through meta-train and meta-test, thereby effectively generalizing to unseen domains.

investigate the application of various graph structures in trajectory prediction [5, 31, 47, 51]. Also, generative models such as GAN [11], Diffusions [15, 30], CVAEs [42], and NPNS [6] contribute to capturing the randomness and uncertainty in real-world scenarios.

However, current methods generally perform well within familiar environments but falter in new settings. This limitation primarily arises from an oversight of distribution discrepancies between training and test datasets, coupled with inadequate consideration of trajectory pattern variations across diverse scenarios. Our statistical analysis in Fig. 1(a) highlights significant differences in density, speed, and acceleration across eight scenarios within the SDD dataset [29], particularly in “Gates”, “Little”, and “Nexus”. As shown in Fig. 1(b), we visualize the environment and all pedestrians’ trajectories. When models are predominantly trained on scenarios such as “Little”, typified by rapid, linear pedestrian movement with distinct directional intent, they learn these patterns well. Similarly, in “Nexus”, where pedestrian density is low and movements are generally slower with fewer interactions, models may easily take effect due to the simplicity and consistency of the behavior. However, this learned simplicity can be a hindrance when models encounter more complex settings. If models are consummately trained on the predictable dynamics of “Little” or the sparser interactions

of “Nexus” and then applied to the “Gates” scenario, their predictive accuracy would likely diminish. This is due to insufficient optimization on the complex and erratic trajectory shifts observed in “Gates”, where the dense population of varying agents necessitates frequent and unpredictable path adjustments to evade collisions.

Addressing the aforementioned issue, several studies have employed Domain Adaptation (DA) [4, 24, 52] to bridge the gap between source and target domains by leveraging techniques that ensure feature consistency across domains, such as feature alignment and adversarial training. However, a limitation of DA is its inherent requirement for target domain data during the training phase. As illustrated in Fig. 1(b), the deployed model should be able to generalize to unseen domains without any updating or fine-tuning. Additionally, some research has explored Domain Generalization (DG) [36, 59], aiming to utilize multiple source domains to cultivate models that can perform effectively in new, unseen environments. It typically encompasses strategies like data augmentation, advanced representation learning, and strategic learning policies. Nevertheless, the specific challenges associated with spatio-temporal aspects and labeling within trajectory prediction domains pose constraints on the application of prevalent DG strategies such as Explicit Feature Alignment [23, 28], Causality-Based Methods [20], Invariant Risk Minimization (IRM) [49] and Ensemble Learning [13]. Meta-learning [19, 53], as a model-agnostic learning paradigm, is a novel alternative in this context. It has been widely applied across various challenges including few-shot learning, image generation, and domain generalization.

In this paper, we primarily investigate how to generalize trajectory prediction models to various domains, ensuring robust performance even in unseen domains. Initially, we delve deeply into two critical factors influencing trajectory prediction: the individual intentions and the interactive effects within group motional patterns. These elements endow the model with the capacity to handle complex scenarios. We propose a dual-path model **Dual Trajectory Transformer** (Dual-TT) consisting of **Interacted-Temporal** (IT) and **Temporal-Interacted** (TI) pathways, amalgamating overarching trajectory features with interaction relationships. Building on this foundation, we propose a framework called **Meta-Learning for Generalized Trajectory Prediction** (MGTP), adeptly simulating the transition between source and target domains through strategically reorganizing training data into meta-train and meta-test segments. This methodology facilitates the model’s adaptation to source and target domains via implicit gradient alignment during the training phase. To circumvent the noise and instability arising from the prediction of uncertain trajectory points, we also design a **Serial and Parallel Training** (SPT) strategy. This approach thoroughly computes gradients in both inner and outer loops to avoid converging to local optima. Concur-

rently, to increase the diversity of trajectory samples and thus reduce overfitting, we innovatively introduce the **MetaMix** strategy. In the unified feature space of meta-train and meta-test phases, we leverage probabilistic parameters from a variational encoder to sample multi-domain extra features, thereby enhancing trajectory prediction in the target domain. Our comprehensive methodology is named **MetaTra: Meta-Learning for Generalized Trajectory Prediction in Unseen Domain**. The research contributions can be summarized as follows:

- To the best of our knowledge, our work is the first to apply a meta-learning framework to address the issue of generalization in trajectory prediction. The proposed **Meta-Learning for Generalized Trajectory Prediction** (MGTP) method entails a tailored delineation of tasks for the meta-train and meta-test phases. Concurrently, it incorporates a **Serial and Parallel Training** (SPT) strategy and the **MetaMix** method to augment the stability of the training process.
- We propose a **Dual Trajectory Transformer** (Dual-TT) model, consisting of **Interacted-Temporal** (IT) and **Temporal-Interacted** (TI) pathways, designed to facilitate an integrative evaluation of the individual intention and the interactive effects within group motional patterns.
- Experiments on three trajectory datasets confirm the consistent superiority of our method. We also show that the integration of MGTP can markedly promote the efficacy of various state-of-the-art prediction models.

2. Related Work

Trajectory Prediction. Recognizing the dynamic and complex nature of agent interactions in trajectory prediction, researchers have shifted towards various types of graphs [5, 40, 47, 51] beyond grid-based representations. However, these methods typically utilize a single or sequential path for spatial and temporal modeling. For instance, **Social-STGCNN** [31] creates spatial graphs with GCNs before processing temporal dynamics with TCNs, potentially overlooking important global intent information. Models like **STGAT** [21] and **Social-BiGAT** [25] have enhanced graph-based approaches by incorporating attention mechanisms, using GAT to assign varying weights to different nodes. Nevertheless, such spatial graphs are typically homogeneous, failing to consider that different types of agents can produce distinct influences even at the same distance.

Domain Adaption (DA) and Domain Generalization (DG). DA aligns distributions between training and testing datasets, with **T-GNN** [52] using a domain-adaptation loss function for this purpose. Methods like **HATN** [47] and **OAMF** [46] incorporate hierarchical structures and the **MEKF** algorithm for domain-specific adjustments. Ivanovic’s work [24] suggests **ALPaCA** for the final model layer, but DA’s limitation is its reliance on target domain

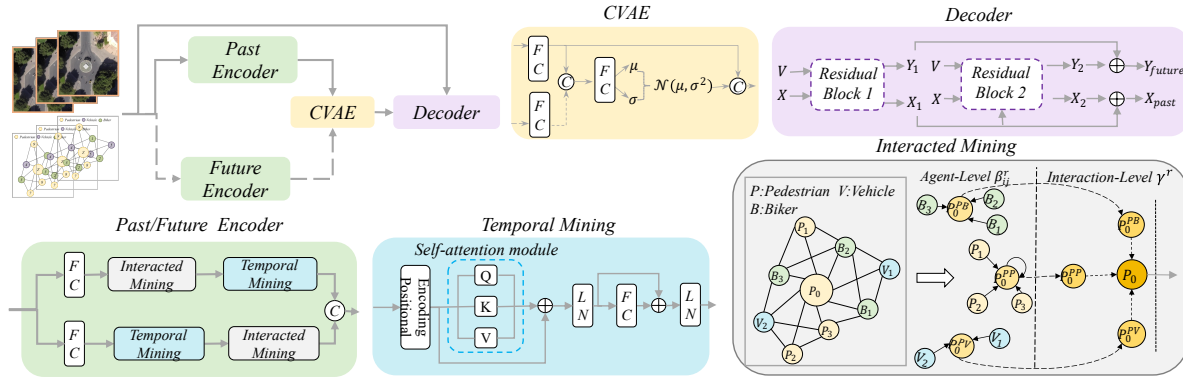


Figure 2. Model architecture of the proposed Dual Trajectory Transformer (Dual-TT).

data. In contrast, DG trains on varied sources for better domain generalization without prior target data. Techniques like data augmentation (rotations, flips, Mixup, CutMix [57]) and adversarial representation learning (CIDDG [28], Diva [23]) enhance training diversity and create domain-agnostic features. AdaRIP [13] is an ensemble learning approach that combines predictions from different models, though it may increase computational demands.

Meta Learning. Meta-learning, known as “learning to learn”, has gained traction with MAML [14] for few-shot learning. Subsequent developments like FOMAML [3] and Reptile [33] simplify second-order gradient computations. ANIL [37] shows that MAML’s effectiveness comes from training approach and feature reuse rather than fine-tuning. Additionally, MLDG [26] expands meta-learning to domain generalization. M³L [58] and MetaMix [53] incorporate knowledge from meta-training to enhance diversity in meta-tests. Lastly, MVDG [34, 56] introduces multi-view regularization to reduce biases and local minima.

3. Method

3.1. Problem Formulation

Assuming the presence of N agents concurrently moving in the scene, we can observe the motion trajectory, denoted as X^i , of the i -th agent over the past t_{obs} moments. The positional coordinates of this trajectory are represented by $X^i = \{o_1^i, \dots, o_{t_{obs}}^i\}$. The orientation of this work is to predict the future trajectory up to time t_{pre} , denoted as $Y^i = \{o_{t_{obs}+1}^i, \dots, o_{t_{pre}}^i\}$. Here, o^i represents the spatial coordinates in either two-dimensional or three-dimensional space.

Particularly, we have access to a dataset comprising N_S source domains $D^S = \{D^1, \dots, D^{N_S}\}$, within which the trajectory prediction model is trained. Concurrently, there is an aspiration for the model to be directly applicable to a target domain D^T emanating from novel environments. Our aim is to develop a predictive model $f(\cdot|\theta)$ endowed with generalizability parameters. For trajectories deriving from unseen domains, the predictive outcome still closely approximates the true values.

3.2. Dual Trajectory Transformer

A generic trajectory prediction model capable of adapting to various scenarios necessitates a comprehensive consideration of multifaceted factors. Precision in predicting the uncertain future trajectories of multi-agents requires a holistic consideration of each agent’s intentions and destinations, which can be approximately inferred from their historically observed trajectories. Additionally, it is essential to consider the impact of various inter-agent relationships on the collective’s overall trajectory patterns. For instance, multiple pedestrians might proceed abreast in the same direction on sidewalks, while athletes on a sports field engage in strategic positioning based on their offensive or defensive roles. In summary, we introduce the Dual Trajectory Transformer (Dual-TT) model (see Fig. 2), which encompasses both Temporal and Interacted Mining components to handle complex scenarios effectively.

Temporal Mining. Trajectory prediction pertains to a sequence prediction problem, where the observed trajectories of agents inform the prognostication of their prospective movement patterns. We employ the classic transformer module to capture the contextual attention in trajectory sequences. This is primarily attributable to the dynamic properties of trajectory data, wherein the prediction of future movement necessitates a simultaneous consideration of both an exhaustive historical representation and their localized patterns. For the initial setup, we offset the input trajectory X with the averaged coordinates of the final observation point, calculating the relative position $o_t^i = o_t^i - \frac{1}{N} \sum_{i=1}^N o_{t_{obs}}^i$ to mitigate the disturbance of scene sizes and absolute coordinate values. Subsequently, the fully connected layer is followed to attain the embedding h^i . The self-attention module sequentially projects the features into a query matrix Q , a key matrix K , and a value matrix V . Thereafter, the dot products between the queries and keys are computed to determine the attention values at various moments, and a weighted sum operator is adopted to aggregate the final temporal feature value h_T^i . This entire process is repeatedly executed with multi-head attention mechanism k times and the outcomes are synthesized.

Interacted Mining. Within the group, agents interact

through multiple relations, with their trajectories giving rise to diverse collective movement patterns, such as the deflection in the travel direction of pedestrians when they are obstructed. Manifestly, the type and magnitude of these interactions necessitate thorough excavation. Some studies [54] have simplified the interactions among all agents yet overlooked the more comprehensive information and rich semantics contained therein.

Inspired by the research of heterogeneous graph neural networks [48], we contemplate the influences each node exerts within the network of disparate interactive relationships. Subsequently, we aggregate the various influential forces impinging upon an agent. For instance, in an NBA match, a player’s movement is predicated not only on giving-and-going with teammates but also on eluding opponents. First of all, we delineate a scenario having R relationship types. Next, we employ the graph attention mechanism to compute the weights of influence between nodes within a specified spatial distance. Given a pair of agents with a relationship r , the significance of their mutual influence is computed by the softmax function as follows:

$$\beta_{ij}^r = \frac{\exp(a_r^T \cdot [h^i || h^j])}{\sum_{k \in \mathcal{N}_i^r} \exp(a_r^T \cdot [h^i || h^k])}, \quad (1)$$

Here, \mathcal{N}_i^r represents the neighbors of node i on the meta-relation r . h^i , h^j and h^k denote the projected features of the nodes, while a_r constitutes the attention vector pertinent to the designated interaction, which is concurrently optimized during the optimization phase. Notably, the influence ratio β_{ij}^r is inherently asymmetric, endowing the inter-agent influences with unidirectional interactions. To thoroughly consider the complexity of relationships, we utilize K-head attention to concatenate learned trajectory features. The semantic features above are ultimately achieved through the aggregation of neighboring nodes.

$$\hat{h}_r^i = \sum_{r=1}^R \sigma \left(\sum_{j \in \mathcal{N}_i^r} \beta_{ij}^r \cdot h^j \right). \quad (2)$$

Ultimately, we can obtain R relation-specific node embeddings for one agent. During the collective motion process, agents often exhibit varying attention towards different relationships. We employ a relational attention vector q , which measures the similarity between each interaction component, to determine the interaction weights. We further normalize these attention weights across all interactions using the softmax function as follows:

$$\gamma^r = \frac{\exp(\frac{1}{N} \sum_{i \in \mathcal{V}} q^T \cdot \tanh(W \cdot \hat{h}_r^i + b))}{\sum_{r=1}^R \exp(\frac{1}{N} \sum_{i \in \mathcal{V}} q^T \cdot \tanh(W \cdot \hat{h}_r^i + b))}. \quad (3)$$

The interaction effects of neighbors can be aggregated using their coefficients as weights for feature fusion:

$$h_{\mathcal{R}}^i = \sum_{r=1}^R \gamma^r \cdot \hat{h}_r^i. \quad (4)$$

Model Framework and Optimization. The aforementioned temporal mining module solely considers the intrinsic patterns of trajectories, lacking an induction of group influence. Conversely, interacted mining mainly focuses on the mutual interactions among nearby agents, yet it tends to overlook the dynamic evolution of trajectories and the agents’ individual intents. To synthesize the strengths of these components, we leverage both sets of features within a dual-path model framework. In the temporal-interacted branch, a temporal mining encoder takes the trajectory coordinates of group members at moments $\{1, \dots, T\}$ as input and then executes interacted mining at time T to yield intermediary features. This process is independently and thoroughly analyzed for each trajectory, culminating in the amalgamation of the comprehensive features of neighboring agents. In the interacted-temporal branch, the influence features between groups at each time are computed separately to explore the interactive impact at that moment. Temporal mining is subsequently applied to obtain the coefficients of these interactive impacts. The concatenation $[h_{\mathcal{T}}^i || h_{\mathcal{R}}^i]$ results in the fused feature embedding for node i (see Fig. 2).

In the prediction phase, we utilize the conditional variational autoencoder (CVAE) model to achieve trajectory probability prediction with a reasonable degree of randomness. Using the observed historical trajectories X , we calculate the conditional probability $P(Y|X)$ for predicting future trajectories \hat{Y} . Additionally, we introduce a latent vector $Z \in \mathcal{R}^{N*d}$ where N and d represent the number and dimension of samples, subsequently compute the posterior probability distribution of future trajectories.

$$p(Y|X) = \int p(Y|X, Z)p(Z|X)dZ. \quad (5)$$

Here, $p(Z|X)$ follows a Gaussian distribution while $p(Y|X, Z)$ is the conditional probability distribution based on X and Z . In order to solve the above equation, we use the evidence lower bound (ELBO) to calculate the loss L_{pred} based on the maximum likelihood estimation method.

$$L_{pred} = -\mathbb{E}_{q(Z|X, Y)} p(Y|X) + KL(q(Z|X, Y) || p(Z|X)). \quad (6)$$

Inspired by Hypertron [43], we utilize a past encoder to model $p(Z|X)$ based on historical trajectories, while also using a future decoder $q(Z|X, Y)$ to model both past and future trajectories. As for $q(Y|X)$, we use residual decoders which both reconstruct past sequences and predict future sequences. During the training phase, the past and future trajectories are separately encoded and concatenated using the proposed Dual-TT module. Two separate perceptrons are used to obtain the parameters μ and σ for sampling $q(Z|X, Y) = \mathcal{N}(\mu_q, \sigma_q)$, which is then acquired by the Gumbel Softmax. During the testing phase, Z is only sampled by $p(Z|X) = \mathcal{N}(\mu_p, \sigma_p)$. Afterwards, Z is concatenated with the past trajectory features and input together with the historical trajectory X into the residual decoders [10], which contain two GRU-MLP encoder-decoder modules, to

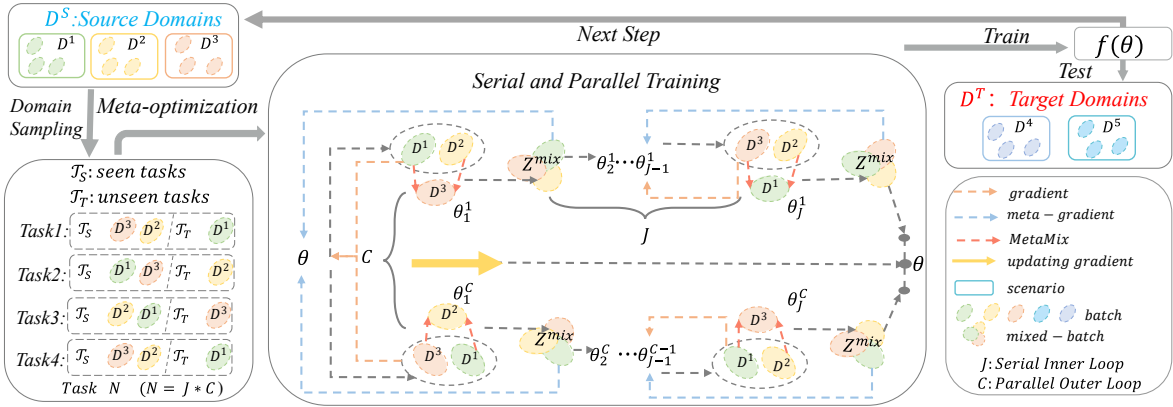


Figure 3. Meta-learning framework for Generalized Trajectory Prediction (MGTP).

obtain the reconstructed and predicted trajectories. We define our overall loss by integrating the evidence lower bound with the deviation between the predicted reconstructed trajectories \hat{X} , future trajectories \hat{Y} , and their actual real-world counterparts X and Y . The formulation is as follows:

$$L = \|\hat{Y} - Y\| + \zeta \cdot KL(q(Z|X, Y) \| p(Z|X)) + \eta \cdot \|\hat{X} - X\|. \quad (7)$$

Compared to Previous Work. Our methodology aligns with prior studies like STAR [54] and STT [32] in employing the attention-based transformer mechanism. Yet, we innovate by implementing symmetrical dual structures for feature fusion. Similar to SGCN [40], our model extracts trajectories from both temporal and spatial perspectives. However, we have developed a more detailed characterization of diverse interaction semantics, complemented by the integration of a more sophisticated decoder.

3.3. Generalized Trajectory Prediction

We now turn our attention to the objective of training a trajectory prediction model $f(\cdot|\theta)$ on the samples from the source domain D^S , and then achieve generalization on the target domain D^T . Intuitively, this objective can be achieved by optimizing the model parameters using losses L_S and L_T derived from the above source and target domains.

$$\sum_{(x^i, y^i) \in D^S} L_S(x^i, y^i; \theta) + \sum_{(x^j, y^j) \in D^T} L_T(x^j, y^j; \theta). \quad (8)$$

Based on this, we introduce the Meta-Learning for Generalized Trajectory Prediction (MGTP) framework (see Fig. 3), which primarily comprises the following components.

Meta-Learning for Unseen Domain. To facilitate trajectory prediction in unseen domains, it is crucial that the feature distribution demonstrates substantial generalizability. Meta-learning is commonly utilized to optimize the learning process, mainly when training samples are limited. A classic paradigm within meta-learning involves adopting an initialization-differentiation methodology across multiple tasks, exemplified by the Model-Agnostic Meta-Learning (MAML). This approach involves iterative gradient updates—both inner and outer loops—to derive initial parameters that can be rapidly fine-tuned across various domains. As an advancement, Reptile employs first-order gradient

updates to enhance the efficiency of the learning process.

Given the unknown feature space of trajectories in the test phase, we employ a cyclic two-order meta-learning approach to replicate the generalization process. As detailed previously, during the meta-training phase, we select $|D^S| - 1$ domains as source domains for a first-order parameter update. Using the loss defined earlier, the temporary parameters θ' can be represented as $\theta' = \theta - \lambda_S \nabla_{\theta} L_S(X, Y; \theta)$. Subsequently, in the meta-testing phase, we compute the loss $L_T(X, Y; \theta')$ using θ' on the target domain to efficaciously enhance the model's generalization capability. The final step involves updating the original parameters θ using a combined loss. This methodology allows to optimize for generalization, where the update process can be concisely delineated as follows.

$$\theta = \theta - (\lambda_S \nabla_{\theta} L_S(X^S, Y^S; \theta) + \lambda_T \nabla_{\theta} L_T(X^T, Y^T; \theta')) \quad (9)$$

The amalgamation of gradients from both directions fosters a trajectory predictor, trained across source and target domains, to derive mutual benefits.

Serial and Parallel Training. Through synergistic gradient optimization across source training domains, the proposed meta-learning module accomplishes model generalization in out-of-domain contexts. However, intuitively, trajectory prediction diverges from classification tasks in that its solution space within various scenes cannot be fully delineated. Gradient updates confined to a single target domain are prone to introducing noise and adversely impacting model stability. Additionally, sparse cross-domain training may make the model ensnare in the local minimum. We propose a training strategy that combines serial and parallel training routes (called Serial and Parallel Training) to address these challenges. In the inner loop, isolated gradient updates do not guarantee comprehensive parameter optimization and may culminate in a suboptimal local minimum. Drawing on the Reptile training methodology, we aim for the trajectory predictor $f(\cdot|\theta)$ to converge towards a solution proximal to each task's manifold of optimal solutions. Consequently, we devise a serial inner loop, repeatedly samples seen tasks τ_S and unseen tasks τ_T within the source domain D^S . Us-

ing gradient descent for parameter updates, we define the parameter updating operation as follows.

$$U_i(\theta_i) = \theta_{i-1} - \lambda(L_{\tau_S^i}(\theta_{i-1}) + L_{\tau_T^i}(\theta_{i-1} - \lambda(L_{\tau_S^i}(\theta_{i-1})))) \quad (10)$$

Upon completion of J serial updates through the operation U_J , the optimized parameters $\tilde{\theta}_J$ for this serial trajectory are obtained. Regarding the original parameters θ_0 , the updating is executed using $\theta_0 = \theta_0 + \kappa(\tilde{\theta}_J - \theta_0)$.

Similarly, for the outer loop, if one were to rely solely on single-view sampling within the outer loop, this would represent merely a transient observational state, highly susceptible to noise and instability. Previous methodologies, such as MVDG [56], have highlighted that optimization in a single direction could lead to inaccuracies, and the resulting sharp minima may compromise generalizability. Inspired by them, we adopt a parallel outer loop approach to comprehensively explore the optimal position within the parameter space. In each iteration, multiple parameter sets $\{\tilde{\theta}_J^1, \dots, \tilde{\theta}_J^C\}$ are obtained. Ultimately, this paper employs an averaging method for parallel updating of parameter values:

$$\theta = \theta + \kappa\left(\sum_{c=1}^C \frac{1}{C} \tilde{\theta}_J^c - \theta\right). \quad (11)$$

Domain Feature Augmentation. Our meta-learning framework emulates the generalization process by performing parameter updates across source and target domains, thereby getting a trajectory predictor applicable in the unseen domain. During this process, as the meta-test phase utilizes tasks from only a single test domain, effectively enhancing the diversity of its samples is conducive to augmenting the model’s generalization capability [41]. However, gathering sufficient target-domain training samples is often impractical. Given that the source domain encompasses a more varied and optimized distribution of feature information, we propose MetaMix, a method to enrich target domain trajectory samples using source domain data. As depicted in Fig. 3, during the meta-test phase, we implement a mixup procedure combining trajectory features from the test domain with those from the source domain. These inter-domain features assist in enhancing the diversity of the features.

Delving specifically into the proposed model, we utilize a gaussian prior distribution during the training process to sample latent embedding Z within mean μ and variation δ . In the meta-training process, $P(Z|X^S, Y^S)$ represents the integrated high-level features originating from the source domain, as opposed to specific sample features. Naturally, in the meta-testing phase, MetaMix aims to resample extra features from this distribution and inject them into the target dataset. For each batch of \mathcal{B} trajectories from the test domain, with latent features $\{Z_i^T\}_{i=1}^{\mathcal{B}}$ obtained from variational encoder, we aim to resample corresponding additional features $\{Z_i^{add}\}_{i=1}^{\mathcal{B}}$ from the source domain, resulting in the mixed features $\{Z_i^{mix}\}_{i=1}^{\mathcal{B}}$. The feature fusion process initi-

ates by sampling a mixing coefficient $\rho \sim Beta(1, 1)$, and simultaneously generating $\{Z_i^{add}\}_{i=1}^{\mathcal{B}}$ from a normal distribution $\mathcal{N}(\mu^S, \delta^S)$. The following formula can encapsulate the calculation process:

$$Z^{mix} = Z^T + (1 - \rho)Z^{add}. \quad (12)$$

During the meta-testing phase, we concatenate the mixup-enhanced latent embeddings Z^{mix} with the initial input Z^T of the decoder, culminating in $2\mathcal{B}$ predicted trajectories as outputted by the decoder. Concurrently, we replicate the true past and future samples from the test tasks, which are then correspondingly employed to compute the test loss.

4. Experiments and Analysis

4.1. Experimental Setup

We evaluate our method on three real-world public datasets: ETH-UCY [54], SDD [22] and NBA [51]. Each training batch includes 512 agents, spanning various time frames, with training 500 epochs. The hyperparameters for the serial inner loop learning rate λ and parallel outer loop learning rate κ are initially set to 0.0015, 0.001. Our method includes 4 parallel optimization paths, each with 4 different serial tasks. We repeat the experiments 5 times and calculate the average to ensure stable results. Details about datasets, baselines, and additional analyses can be found in the Appendix.

4.2. Prediction Performance

ETH-UCY Dataset. In Table 1, we compare our approach with several commonly used methods. To compare with AgentFormer, our method improves the average minADE₂₀ from 0.23 to 0.21. Additionally, our method consistently achieves the best or second-best performance across various sub-scenarios. Particularly in the ETH scenario, where many conventional methods falter, our approach significantly reduces the minADE₂₀ from 0.45 to 0.25, representing an efficiency gain of nearly 45%. By incorporating our MGTP into the AgentFormer model, we achieve a significant performance improvement, resulting in an 8.6% reduction in minADE₂₀ and a 10.2% reduction in minFDE₂₀.

To investigate the underlying factors contributing to the underperformance of conventional methods in the ETH scenario, we collect metrics related to pedestrian density, speed and acceleration. As shown in Fig. 4a, the ETH scenario exhibits the lowest pedestrian density while displaying notably higher average speed and acceleration when compared to other scenarios. This highlights significant disparities between the ETH scenario and the rest. To further analyze, we employ T-SNE [44] visualization. Without the MGTP framework, as shown in Fig. 4b, the “zara1” and “zara2” scenarios exhibit overlapping features, indicating similar trajectory designs and spatial distributions. The “univ” and “hotel” scenarios have a wider feature distribution, with some

Table 1. minADE₂₀/minFDE₂₀ (meters) results on ETH-UCY. Agent Former performs best in previous methods (marked with *) and gets better when utilizing MGTP as a plugin. Our Dual-TT, integrated with MGTP, achieves the best results. (bold: best, underline: runner-up)

Subset	Social-STGCNN CVPR20[31]	Trajectron++ ECCV20[39]	PECNet ECCV20[29]	STAR ECCV20[54]	GroupNet CVPR22[51]	Agent Former* ICCV21[55]	Agent Former* +MGTP	Dual-TT	Dual-TT +MGTP
ETH	0.64/1.11	0.61/1.02	0.54/0.87	0.36/0.65	0.46/0.73	0.45/0.75	0.36/0.57	<u>0.29/0.54</u>	0.24/0.46
HOTEL	0.49/0.85	0.19/0.28	0.18/0.24	0.21/0.41	0.15/0.25	0.14/0.22	0.13/0.21	0.15/0.28	<u>0.13/0.23</u>
UNIV	0.44/0.79	0.30/0.54	0.35/0.60	0.33/0.67	0.26/0.45	<u>0.25/0.45</u>	0.24/0.43	0.31/0.61	0.29/0.58
ZARA1	0.34/0.53	0.24/0.42	0.22/0.39	0.29/0.52	0.21/0.39	0.18/0.30	0.19/0.30	0.23/0.46	<u>0.18/0.39</u>
ZARA2	0.30/0.48	0.18/0.32	0.17/0.30	0.22/0.46	0.17/0.33	<u>0.14/0.24</u>	0.13/0.22	0.19/0.38	0.16/0.33
AVG	0.44/0.75	0.30/0.51	0.29/0.48	0.28/0.54	0.25/0.44	0.23/0.39	<u>0.21/0.35</u>	0.23/0.45	0.20/0.40

Table 2. minADE₂₀/minFDE₂₀ (pixels) results on SDD. PECNet performs best in previous methods (marked with *) and gets better when utilizing MGTP as a plugin. Our Dual-TT, integrated with MGTP, achieves the best results. (bold: best, underline: runner-up)

agents type	Social-STGCNN CVPR20[31]	Trajectron++ ECCV20[39]	STAR ECCV20[54]	Agent Former ICCV21[55]	Group Net CVPR22[51]	PECNet* ECCV20[29]	PECNet* +MGTP	Dual-TT	Dual-TT +MGTP
pedestrian	20.25/35.75	19.30/32.70	17.63/36.21	10.32/18.30	9.31/16.11	9.96/15.88	<u>8.91/13.38</u>	12.79/15.88	8.49/11.85
all-agents	27.23/41.44	25.66/39.76	27.73/52.37	16.84/29.82	14.05/27.67	14.18/24.47	<u>10.97/18.40</u>	16.27/29.38	10.13/17.05

interspersed between “zara1” and “zara2”, while others form distinct clusters. Features in the ETH scenario are distinctly isolated from those in the other four scenarios, leading to discrepancies between decoded trajectories and actual values, resulting in lower model performance. However, with the integration of MGTP framework, as shown in Fig. 4c, feature distribution aligns across scenarios, demonstrating improved generalization capabilities.

SDD Dataset. When applying previous methodologies to this dataset, it results in the creation of two distinct testing configurations. One configuration focuses exclusively on pedestrians, while the other encompasses all types of intelligent agents. To ensure a thorough comparison, we conduct tests under both configurations. According to our findings presented in Table 2, the integration of the Dual-TT with the MGTP outperforms other methods, resulting in a 12.5% decrease in the minADE₂₀ metric compared to PecNet. Additionally, by incorporating the MGTP into the PecNet, we achieve performance improvement, leading to a 10.5% reduction in minADE₂₀ and a 9.44% reduction in minFDE₂₀. Furthermore, we adopt a leave-one-out strategy, similar to the ETH-UCY dataset, to revise the partitioning of the SDD dataset. This allows us to conduct additional experiments with Dual-TT model and MGTP framework under new configurations. Our comprehensive findings, shown in Fig. 4d, consistently demonstrate improved predictive accuracy across all scenarios. Particularly noteworthy are the significant improvements observed in the “Gates”, “Little”, and “DeathCircle” scenarios, highlighting the effectiveness of the MGTP framework in specific contexts.

NBA Dataset. Our experimental results, as shown in Table 3, demonstrate that our method consistently outperforms existing techniques across all timestamps in the NBA dataset.

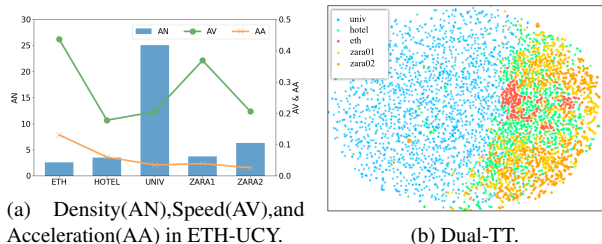


Figure 4. Detail analysis for ETH-UCY and SDD.

When compared to the leading baseline method GroupNet, we achieve a significant 14.5% reduction in minADE₂₀. Furthermore, by integrating the MGTP with GroupNet, we observe respective decreases of 3.7% and 6.9% in minADE₂₀ and minFDE₂₀.

We adopt a meta-training and meta-testing partition strategy based on home teams when applying the MGTP framework. This decision is motivated by the consistent geographic scenario observed in the NBA dataset, where athletes exhibit distinct group behavior. Unlike previous pedestrian datasets, the NBA dataset demonstrates cohesive actions among team members, with high interdependencies in their behaviors and trajectories. Notable variations can be observed across different teams, particularly in their offensive and defensive playstyles. We extract samples from the primary NBA dataset, focusing on teams such as CLE, GSW, NYK, OKC, and SAS. Through leave-one-out experiments, as shown in Fig. 5a and Fig. 5b, we consistently observe performance improvements for the Dual-TT model integrated with the MGTP framework when evaluating on these teams as test sets. These results affirm the robustness of the MGTP framework, which organizes the training dataset based on distinct home teams, thereby enhancing model generalization capabilities.

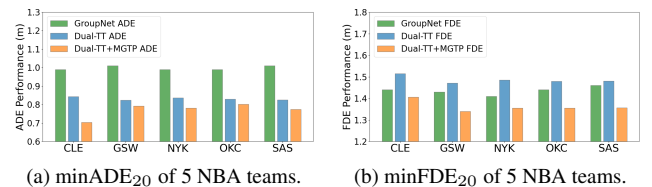


Figure 5. Performance metrics for 5 NBA teams.

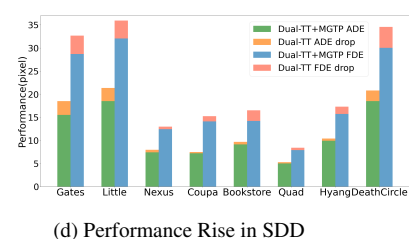


Table 3. minADE₂₀/minFDE₂₀ (meters) results on NBA. GroupNet performs best in previous methods (marked with *) and gets better when utilizing MGTP as a plugin. Our Dual-TT, integrated with MGTP, achieves the best results. (bold: best, underline: runner-up)

Time	Social-STGCNN CVPR20[31]	Trajectron++ ECCV20[39]	Agent Former ICCV21[55]	STAR ECCV20[54]	PECNet ECCV20[29]	GroupNet* CVPR22[51]	GroupNet* +MGTP	Dual-TT	Dual-TT +MGTP
1.0s	0.41/0.62	0.30/0.38	0.45/0.64	0.43/0.66	0.40/0.71	0.26/0.34	<u>0.25/0.32</u>	0.26/0.39	0.23/0.35
2.0s	0.81/1.32	0.59/0.82	0.84/1.44	0.75/1.24	0.83/1.61	0.49/0.70	0.46/0.66	<u>0.44/0.71</u>	0.42/0.60
3.0s	1.19/1.94	0.85/1.24	1.24/2.18	1.03/1.51	1.27/2.44	0.73/1.02	0.70/0.97	<u>0.67/1.23</u>	0.64/0.92
4.0s	1.59/2.41	1.15/1.57	1.62/2.84	1.13/2.01	1.69/2.95	0.96/1.30	0.93/1.21	<u>0.87/1.45</u>	0.82/1.37

Table 4. minADE₂₀/minFDE₂₀ (meters) results of different MGTP variants on the ETH-UCY dataset.

ML	SPT	MM	ETH	HOTEL	UNIV	ZARA1	ZARA2	AVG
×	×	×	0.289/0.544	0.153/0.281	0.315/0.612	0.233/0.475	0.188/0.378	0.2356/0.4580
✓	×	×	0.279/0.536	0.147/0.280	0.305/0.606	0.213/0.414	0.184/0.380	0.2263/0.4532
✓	✓	×	0.258/0.491	0.136/0.240	0.292/0.590	0.189/0.396	0.169/0.343	0.2088/0.4120
✓	✓	✓	0.245/0.465	0.130/0.233	0.290/0.586	0.184/0.392	0.162/0.332	0.2034/0.4034

4.3. Ablation Studies

We compare the performance of MGTP with versions that have specific components removed to assess their impact on the model’s performance. Our findings are detailed in the subsequent section and Table 4:

Meta-Learning Basic Module(ML): According to our observations, we note an overall reduction of 8.8% and 6.8% in the minADE₂₀/minFDE₂₀ metrics, indicating improved performance. This improvement can be primarily attributed to the combined effect of individual losses during bi-level optimization. By aligning gradients in the training phase, this approach ensures consistent gradient updates across domains, leading to enhanced cross-domain performance and reducing overfitting within individual domains.

Serial and Parallel Training(SPT): Our approach combines the principles of parallel multi-perspective, which involves combining various optimization paths, and serial multi-tasks, which integrates different domain tasks. This combination serves two purposes: preventing the model from converging to local optima and promoting a thorough exploration of the weight space. As shown in Table 4, our approach consistently outperforms all baselines in the five scenarios evaluated. Particularly notable are the significant increases in minADE₂₀ for the “eth” and “zara2” scenarios, with improvements of 10.7% and 11.7% respectively.

MetaMix(MM): The implementation of the MetaMix strategy has been proven effective in diversifying the meta-testing domain features, resulting in enhanced generalizability of the model. As presented in Table 4, significant performance improvements can be observed across all scenarios. This highlights the capability of a diverse meta-testing feature set in capturing the complexity and variability of new domains, especially under conditions of domain shift.

4.4. Qualitative Results

Fig. 6 presents the multimodal prediction results across various scenarios in the SDD dataset. It is noteworthy that our proposed model’s predictions closely align with the ground truth trajectories in the majority of scenarios. Even without relying on map-based context, the model demonstrates profi-

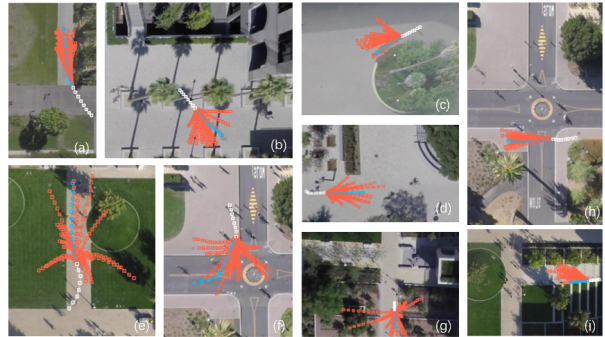


Figure 6. Qualitative examples from SDD: white lines show past trajectories, red lines are predictions from the CVAE decoder, and blue lines represent actual trajectories.

cient navigation around obstacles. For instance, subfigures (a) and (f) show trajectories primarily confined within passable roads, while subfigure (c) exhibits expansion towards obstruction-free areas. In complex scenarios characterized by diverse pedestrian intentions, such as subfigures (e) and (f), the model produces multiple predictions that vary in direction and speed, yet remain plausible. This highlights the effectiveness of our model in generating diverse and realistic predictions in multimodal forecasting tasks.

5. Conclusion

In this paper, we introduce MetaTra, a novel approach to enhance the generalization performance of trajectory prediction models, focusing on two key aspects: (1) the Dual Trajectory Transformer (Dual-TT), a model adept at assimilating assessments of an individual’s intended destination with the dynamics of group motion interactions, and (2) the Meta-Learning for Generalized Trajectory Prediction (MGTP) framework, specifically designed to facilitate trajectory prediction in unseen domain by tuning the training process. Empirical evaluations across several real-world datasets substantiate the efficacy of our approach, showcasing its superior performance in domain generalization. Furthermore, experimental results validate its potential to promote other trajectory prediction models through a plug-and-play unit.

References

- [1] Metrica sports. <https://github.com/metrica-sports>, Apr 16, 2021. 1, 12
- [2] Alexandre Alahi, Kratarth Goel, Vignesh Ramanathan, Alexandre Robicquet, Li Fei-Fei, and Silvio Savarese. Social lstm: Human trajectory prediction in crowded spaces. In *Proceedings of the IEEE conference on computer vision and pattern recognition*, pages 961–971, 2016. 1
- [3] Antreas Antoniou, Harrison Edwards, and Amos Storkey. How to train your maml. *arXiv preprint arXiv:1810.09502*, 2018. 3
- [4] Görkay Aydemir, Adil Kaan Akan, and Fatma Güney. Adapt: Efficient multi-agent trajectory prediction with adaptation. In *Proceedings of the IEEE/CVF International Conference on Computer Vision*, pages 8295–8305, 2023. 2
- [5] Inhwon Bae, Jin-Hwi Park, and Hae-Gon Jeon. Learning pedestrian group representations for multi-modal trajectory prediction. In *European Conference on Computer Vision*, pages 270–289. Springer, 2022. 1, 2
- [6] Inhwon Bae, Jin-Hwi Park, and Hae-Gon Jeon. Non-probability sampling network for stochastic human trajectory prediction. In *Proceedings of the IEEE/CVF Conference on Computer Vision and Pattern Recognition*, pages 6477–6487, 2022. 1
- [7] Richard Bellman. A markovian decision process. *Journal of mathematics and mechanics*, pages 679–684, 1957. 1
- [8] Abderrahmane Boubezoul, Abdourahmane Koita, and Dimitri Daucher. Vehicle trajectories classification using support vectors machines for failure trajectory prediction. In *2009 International Conference on Advances in Computational Tools for Engineering Applications*, pages 486–491. IEEE, 2009. 1
- [9] Adrian Broadhurst, Simon Baker, and Takeo Kanade. Monte carlo road safety reasoning. In *IEEE Proceedings. Intelligent Vehicles Symposium, 2005.*, pages 319–324. IEEE, 2005. 1
- [10] Defu Cao, Yujing Wang, Juanyong Duan, Ce Zhang, Xia Zhu, Congrui Huang, Yunhai Tong, Bixiong Xu, Jing Bai, Jie Tong, et al. Spectral temporal graph neural network for multivariate time-series forecasting. *Advances in neural information processing systems*, 33:17766–17778, 2020. 4
- [11] Patrick Dendorfer, Sven Elflein, and Laura Leal-Taixé. Mgan: A multi-generator model preventing out-of-distribution samples in pedestrian trajectory prediction. In *Proceedings of the IEEE/CVF International Conference on Computer Vision*, pages 13158–13167, 2021. 1
- [12] Qi Deng and Dirk Söfker. Improved driving behaviors prediction based on fuzzy logic-hidden markov model (fl-hmm). In *2018 IEEE Intelligent Vehicles Symposium (IV)*, pages 2003–2008. IEEE, 2018. 1
- [13] Angelos Filos, Panagiotis Tigkas, Rowan McAllister, Nicholas Rhinehart, Sergey Levine, and Yarín Gal. Can autonomous vehicles identify, recover from, and adapt to distribution shifts? In *International Conference on Machine Learning*, pages 3145–3153. PMLR, 2020. 2, 3
- [14] Chelsea Finn, Pieter Abbeel, and Sergey Levine. Model-agnostic meta-learning for fast adaptation of deep networks. In *International conference on machine learning*, pages 1126–1135. PMLR, 2017. 3
- [15] Tianpei Gu, Guangyi Chen, Junlong Li, Chunze Lin, Yongming Rao, Jie Zhou, and Jiwen Lu. Stochastic trajectory prediction via motion indeterminacy diffusion. In *Proceedings of the IEEE/CVF Conference on Computer Vision and Pattern Recognition*, pages 17113–17122, 2022. 1
- [16] Agrim Gupta, Justin Johnson, Li Fei-Fei, Silvio Savarese, and Alexandre Alahi. Social gan: Socially acceptable trajectories with generative adversarial networks. In *Proceedings of the IEEE conference on computer vision and pattern recognition*, pages 2255–2264, 2018. 1, 12
- [17] Ganglei He, Xin Li, Ying Lv, Bingzhao Gao, and Hong Chen. Probabilistic intention prediction and trajectory generation based on dynamic bayesian networks. In *2019 Chinese Automation Congress (CAC)*, pages 2646–2651. IEEE, 2019. 1
- [18] Jonathan Ho and Stefano Ermon. Generative adversarial imitation learning. *Advances in neural information processing systems*, 29, 2016. 1
- [19] Timothy Hospedales, Antreas Antoniou, Paul Micaelli, and Amos Storkey. Meta-learning in neural networks: A survey. *IEEE transactions on pattern analysis and machine intelligence*, 44(9):5149–5169, 2021. 2
- [20] Yeping Hu, Xiaogang Jia, Masayoshi Tomizuka, and Wei Zhan. Causal-based time series domain generalization for vehicle intention prediction. In *2022 International Conference on Robotics and Automation (ICRA)*, pages 7806–7813. IEEE, 2022. 2
- [21] Yingfan Huang, Huikun Bi, Zhaoxin Li, Tianlu Mao, and Zhaoqi Wang. Stgat: Modeling spatial-temporal interactions for human trajectory prediction. In *Proceedings of the IEEE/CVF international conference on computer vision*, pages 6272–6281, 2019. 2
- [22] Bo Hui, Da Yan, Haiquan Chen, and Wei-Shinn Ku. Trajnet: A trajectory-based deep learning model for traffic prediction. In *Proceedings of the 27th ACM SIGKDD Conference on Knowledge Discovery & Data Mining*, pages 716–724, 2021. 6, 12
- [23] Maximilian Ilse, Jakub M Tomczak, Christos Louizos, and Max Welling. Diva: Domain invariant variational autoencoders. In *Medical Imaging with Deep Learning*, pages 322–348. PMLR, 2020. 2, 3
- [24] Boris Ivanovic, James Harrison, and Marco Pavone. Expanding the deployment envelope of behavior prediction via adaptive meta-learning. In *2023 IEEE International Conference on Robotics and Automation (ICRA)*, pages 7786–7793. IEEE, 2023. 2
- [25] Vineet Kosaraju, Amir Sadeghian, Roberto Martín-Martín, Ian Reid, Hamid Rezaatofghi, and Silvio Savarese. Socialbigat: Multimodal trajectory forecasting using bicycle-gan and graph attention networks. *Advances in Neural Information Processing Systems*, 32, 2019. 2
- [26] Da Li, Yongxin Yang, Yi-Zhe Song, and Timothy Hospedales. Learning to generalize: Meta-learning for domain generalization. In *Proceedings of the AAAI conference on artificial intelligence*, 2018. 3
- [27] Jiachen Li, Fan Yang, Masayoshi Tomizuka, and Chiho Choi. Evolvegraph: Multi-agent trajectory prediction with dynamic

- relational reasoning. *Advances in neural information processing systems*, 33:19783–19794, 2020. [1](#), [12](#)
- [28] Ya Li, Xinmei Tian, Mingming Gong, Yajing Liu, Tongliang Liu, Kun Zhang, and Dacheng Tao. Deep domain generalization via conditional invariant adversarial networks. In *Proceedings of the European conference on computer vision (ECCV)*, pages 624–639, 2018. [2](#), [3](#)
- [29] Karttikeya Mangalam, Harshayu Girase, Shreyas Agarwal, Kuan-Hui Lee, Ehsan Adeli, Jitendra Malik, and Adrien Gaidon. It is not the journey but the destination: Endpoint conditioned trajectory prediction. In *Computer Vision–ECCV 2020: 16th European Conference, Glasgow, UK, August 23–28, 2020, Proceedings, Part II 16*, pages 759–776. Springer, 2020. [1](#), [7](#), [8](#), [12](#), [13](#)
- [30] Weibo Mao, Chenxin Xu, Qi Zhu, Siheng Chen, and Yanfeng Wang. Leapfrog diffusion model for stochastic trajectory prediction. In *Proceedings of the IEEE/CVF Conference on Computer Vision and Pattern Recognition*, pages 5517–5526, 2023. [1](#)
- [31] Abdullh Mohamed, Kun Qian, Mohamed Elhoseiny, and Christian Claudel. Social-stgcn: A social spatio-temporal graph convolutional neural network for human trajectory prediction. In *Proceedings of the IEEE/CVF conference on computer vision and pattern recognition*, pages 14424–14432, 2020. [1](#), [2](#), [7](#), [8](#), [12](#)
- [32] Alessio Monti, Angelo Porrello, Simone Calderara, Pasquale Coscia, Lamberto Ballan, and Rita Cucchiara. How many observations are enough? knowledge distillation for trajectory forecasting. In *Proceedings of the IEEE/CVF Conference on Computer Vision and Pattern Recognition*, pages 6553–6562, 2022. [5](#)
- [33] Alex Nichol, Joshua Achiam, and John Schulman. On first-order meta-learning algorithms. *arXiv preprint arXiv:1803.02999*, 2018. [3](#)
- [34] Li Niu, Wen Li, and Dong Xu. Multi-view domain generalization for visual recognition. In *Proceedings of the IEEE international conference on computer vision*, pages 4193–4201, 2015. [3](#)
- [35] Shao-jie QIAO, Nan Han, Xin-wen ZHU, Hong-ping SHU, Jiao-ling ZHENG, and Chang-an YUAN. A dynamic trajectory prediction algorithm based on kalman filter. *Acta Electronica Sinica*, 46(2):418, 2018. [1](#)
- [36] Xin Qin, Jindong Wang, Yiqiang Chen, Wang Lu, and Xinlong Jiang. Domain generalization for activity recognition via adaptive feature fusion. *ACM Transactions on Intelligent Systems and Technology*, 14(1):1–21, 2022. [2](#)
- [37] Aniruddh Raghu, Maithra Raghu, Samy Bengio, and Oriol Vinyals. Rapid learning or feature reuse? towards understanding the effectiveness of maml. *arXiv preprint arXiv:1909.09157*, 2019. [3](#)
- [38] Amir Sadeghian, Vineet Kosaraju, Ali Sadeghian, Noriaki Hirose, Hamid Rezafofighi, and Silvio Savarese. Sophie: An attentive gan for predicting paths compliant to social and physical constraints. In *Proceedings of the IEEE/CVF conference on computer vision and pattern recognition*, pages 1349–1358, 2019. [1](#), [12](#)
- [39] Tim Salzmann, Boris Ivanovic, Punarjay Chakravarty, and Marco Pavone. Trajectron++: Dynamically-feasible trajectory forecasting with heterogeneous data. In *Computer Vision–ECCV 2020: 16th European Conference, Glasgow, UK, August 23–28, 2020, Proceedings, Part XVIII 16*, pages 683–700. Springer, 2020. [7](#), [8](#), [12](#)
- [40] Liushuai Shi, Le Wang, Chengjiang Long, Sanping Zhou, Mo Zhou, Zhenxing Niu, and Gang Hua. Sgcn: Sparse graph convolution network for pedestrian trajectory prediction. In *Proceedings of the IEEE/CVF Conference on Computer Vision and Pattern Recognition*, pages 8994–9003, 2021. [2](#), [5](#)
- [41] Yang Shu, Zhangjie Cao, Chenyu Wang, Jianmin Wang, and Mingsheng Long. Open domain generalization with domain-augmented meta-learning. In *Proceedings of the IEEE/CVF conference on computer vision and pattern recognition*, pages 9624–9633, 2021. [6](#)
- [42] Kihyuk Sohn, Honglak Lee, and Xinchen Yan. Learning structured output representation using deep conditional generative models. *Advances in neural information processing systems*, 28, 2015. [1](#)
- [43] Yu Tian, Xingliang Huang, Ruigang Niu, Hongfeng Yu, Peijin Wang, and Xian Sun. Hypertron: Explicit social-temporal hypergraph framework for multi-agent forecasting. [4](#)
- [44] Laurens Van der Maaten and Geoffrey Hinton. Visualizing data using t-sne. *Journal of machine learning research*, 9(11), 2008. [6](#)
- [45] Ashish Vaswani, Noam Shazeer, Niki Parmar, Jakob Uszkoreit, Llion Jones, Aidan N Gomez, Łukasz Kaiser, and Illia Polosukhin. Attention is all you need. *Advances in neural information processing systems*, 30, 2017. [1](#)
- [46] Letian Wang, Yeping Hu, and Changliu Liu. Online adaptation of neural network models by modified extended kalman filter for customizable and transferable driving behavior prediction. *arXiv preprint arXiv:2112.06129*, 2021. [2](#)
- [47] Letian Wang, Yeping Hu, Liting Sun, Wei Zhan, Masayoshi Tomizuka, and Changliu Liu. Transferable and adaptable driving behavior prediction. *arXiv preprint arXiv:2202.05140*, 2022. [1](#), [2](#)
- [48] Xiao Wang, Houye Ji, Chuan Shi, Bai Wang, Yanfang Ye, Peng Cui, and Philip S Yu. Heterogeneous graph attention network. In *The world wide web conference*, pages 2022–2032, 2019. [4](#)
- [49] Yunkai Wang, Dongkun Zhang, Yuxiang Cui, Zexi Chen, Wei Jing, Junbo Chen, Rong Xiong, and Yue Wang. Domain generalization for vision-based driving trajectory generation. In *2022 International Conference on Robotics and Automation (ICRA)*, pages 8950–8956. IEEE, 2022. [2](#)
- [50] Yuning Wang, Pu Zhang, Lei Bai, and Jianru Xue. Fend: A future enhanced distribution-aware contrastive learning framework for long-tail trajectory prediction. In *Proceedings of the IEEE/CVF Conference on Computer Vision and Pattern Recognition*, pages 1400–1409, 2023. [1](#)
- [51] Chenxin Xu, Maosen Li, Zhenyang Ni, Ya Zhang, and Siheng Chen. Groupnet: Multiscale hypergraph neural networks for trajectory prediction with relational reasoning. In *Proceedings of the IEEE/CVF Conference on Computer Vision and Pattern Recognition*, pages 6498–6507, 2022. [1](#), [2](#), [6](#), [7](#), [8](#), [12](#), [13](#)
- [52] Yi Xu, Lichen Wang, Yizhou Wang, and Yun Fu. Adaptive trajectory prediction via transferable gnn. In *Proceedings of*

- the IEEE/CVF Conference on Computer Vision and Pattern Recognition*, pages 6520–6531, 2022. 2
- [53] Huaxiu Yao, Long-Kai Huang, Linjun Zhang, Ying Wei, Li Tian, James Zou, Junzhou Huang, et al. Improving generalization in meta-learning via task augmentation. In *International conference on machine learning*, pages 11887–11897. PMLR, 2021. 2, 3
- [54] Cunjun Yu, Xiao Ma, Jiawei Ren, Haiyu Zhao, and Shuai Yi. Spatio-temporal graph transformer networks for pedestrian trajectory prediction. In *Computer Vision–ECCV 2020: 16th European Conference, Glasgow, UK, August 23–28, 2020, Proceedings, Part XII 16*, pages 507–523. Springer, 2020. 4, 5, 6, 7, 8, 12, 13
- [55] Ye Yuan, Xinshuo Weng, Yanglan Ou, and Kris M Kitani. Agentformer: Agent-aware transformers for socio-temporal multi-agent forecasting. In *Proceedings of the IEEE/CVF International Conference on Computer Vision*, pages 9813–9823, 2021. 7, 8, 12
- [56] Jian Zhang, Lei Qi, Yinghuan Shi, and Yang Gao. Mvdg: A unified multi-view framework for domain generalization. In *European Conference on Computer Vision*, pages 161–177. Springer, 2022. 3, 6
- [57] Linjun Zhang, Zhun Deng, Kenji Kawaguchi, Amirata Ghorbani, and James Zou. How does mixup help with robustness and generalization? *arXiv preprint arXiv:2010.04819*, 2020. 3
- [58] Yuyang Zhao, Zhun Zhong, Fengxiang Yang, Zhiming Luo, Yaojin Lin, Shaozi Li, and Nicu Sebe. Learning to generalize unseen domains via memory-based multi-source meta-learning for person re-identification. In *Proceedings of the IEEE/CVF conference on computer vision and pattern recognition*, pages 6277–6286, 2021. 3
- [59] Kaiyang Zhou, Ziwei Liu, Yu Qiao, Tao Xiang, and Chen Change Loy. Domain generalization: A survey. *IEEE Transactions on Pattern Analysis and Machine Intelligence*, 2022. 2

A. MGTP Algorithmic

The complete learning process of MGTP is summarized in Algorithm 1.

Algorithm 1 Meta-Learning for Generalized Trajectory Prediction (MGTP).

```

1: Input: source data  $D^S = \{D_1^S, \dots, D_N^S\}$ ;
2: Init: network parametrized by  $\theta$ , serial inner loop learning rate  $\lambda$ , parallel outer loop learning rate  $\kappa$ , the number of parallel optimization parameter set  $C$ , the number of serial sampled task  $J$ ;
3: while not converged do
4:   for  $c = 1$  to  $C$  do
5:      $\theta_0^c \leftarrow$  Initialized by  $\theta$ ;
6:     for  $i = 1$  to  $J$  do
7:       Randomly sample source tasks  $\tau_S$  and
8:       target tasks  $\tau_T$  within the source domains
9:        $D^S$ ;
10:      Meta-Train:
11:      Compute meta-train loss  $L_{\tau_S^i}(\theta_{i-1}^c)$  and
12:      compute the temporary parameters:
13:       $\theta'_{i-1}^c \leftarrow \theta_{i-1}^c - \lambda(L_{\tau_S^i}(\theta_{i-1}^c))$ ;
14:      Meta-test:
15:      Diversify meta-test features with MetaMix;
16:      Compute meta-test loss  $L_{\tau_T^i}(\theta'_{i-1}^c)$ ;
17:    end for
18:    Serial Inner Optimization:
19:     $\theta_i^c \leftarrow \theta_{i-1}^c - \lambda(L_{\tau_S^i}(\theta_{i-1}^c) + L_{\tau_T^i}(\theta'_{i-1}^c))$ ;
20:  end for
21:  Get the parallel optimization parameter set
22:   $\{\tilde{\theta}_J^1, \dots, \tilde{\theta}_J^C\}$ ;
23:  Parallel Outer Optimization:
24:   $\theta \leftarrow \theta + \kappa(\sum_{c=1}^C \frac{1}{C} \tilde{\theta}_J^c - \theta)$ .
25: end while

```

B. Experiments

B.1. Datasets and Preprocessing

- **ETH-UCY Dataset [39]:** This dataset contains five campus scenarios: ETH, HOTEL, UNIV, ZARA1, and ZARA2, segmenting pedestrian trajectories into 8-second slices. Each slice utilizes an input trajectory of 3.2 seconds (8 frames) to predict a future trajectory spanning 4.8 seconds (12 frames). We select one scenario as the unseen domain for testing by turn while employing the remaining four scenarios for model training, and subsequently calculate the mean of the results.
- **StanfordDrone Dataset (SDD) [16]:** SDD contains approximately 60 videos from 8 primary areas around a university campus, captured via drones. These videos predominantly comprise humans, bikes, and cars. SDD utilizes 3.2

seconds (8 frames) of past data to predict the subsequent 4.8 seconds (12 frames). We follow TrajNet’s settings [22] for fair evaluation, initially focusing on pedestrians as PECNet [29], then expanding to all agents like Sophie [38]. Moreover, each area alternates as the unseen test set, illustrating the effect of MetaTra on generalization.

- **NBA SportVU Dataset (NBA) [27]:** This dataset includes trajectories of NBA players and the ball during the 2015-2016 season, collected from SportVU. We follow GroupNet’s [51] settings for fair evaluation and utilize 2 seconds (5 frames) to forecast the subsequent 4 seconds (10 frames). Additionally, we categorize data into five home team scenarios (CLE, GSW, SAS, OKC, NYK), and in each test, we randomly select one home team as the unseen domain to achieve domain generalization.
- **Soccer Dataset [1]:** The Metrica Sports dataset contains anonymized trackings and event datas, encompassing two games in standard format and one in the EPTS FIFA format. The coordinates in this dataset range from 0 to 1 on each axis, accurately representing the football field of 105x68 meters. Training is conducted on the NBA dataset, with testing on the Soccer dataset, an analogous athletic context, to validate the model’s capability in handling tasks in entirely unseen domains.

B.2. Metrics

We employ two standard metrics: minADE_K and minFDE_K . minADE_K represents the minimum average distance across all corresponding points between the K predicted trajectories and the actual trajectory. Subsequently, minFDE_K denotes the minimum distance between the final destinations of the K predicted trajectories and that of the actual trajectory.

B.3. Comparison Methods

- **STAR [54]:** STAR decomposes the spatio-temporal attention modeling into temporal modeling and spatial modeling. It incorporates a memory module and a self-attention approach, enabling sequential frame-by-frame prediction.
- **GroupNet [51]:** GroupNet captures interactions and undertakes representation learning by operating on a multi-scale hypergraph neural network. It integrates CVAE with residual decoders designed for sequence prediction.
- **Social-STGCNN [31]:** Social-STGCNN employs GCNs to form spatial graphs over time and TCN models for temporal processing.
- **PECNet [29]:** Built upon a social pooling layer, this model employs VAE to estimate potential future endpoints, facilitating subsequent trajectory prediction.
- **Trajectron++ [39]:** This model combines a graph-structured framework with a CVAE-based approach, integrating the InfoVAE objective with agent dynamics for enriched trajectory modeling.
- **AgentFormer [55]:** Featuring a uniquely designed agent-

aware attention mechanism, AgentFormer simultaneously processes temporal and spatial dimensions. It employs CVAE and DLow to generate varied and plausible trajectories.

- **Dual-TT**: We introduce the Dual Trajectory Transformer (Dual-TT) model, which is composed of two pathways: the Interacted-Temporal (IT) and the Temporal-Interacted (TI).
- **MGTP**: We propose the Meta-Learning for Generalized Trajectory Prediction (MGTP) method, which includes an innovative task delineation for the meta-train and meta-test phases. Additionally, it integrates a Serial and Parallel Training (SPT) strategy with the MetaMix method to enhance the stability of the training process.

B.4. NBA-Soccer Transfer

Table 5. [NBA → Soccer] minADE₂₀/minFDE₂₀ (meters) results on NBA-Soccer Transfer settings. Our Dual-TT, integrated with MGTP, achieves the best results. (bold: best, underline: runner-up)

metric	GroupNet	PECNet	STAR	Dual-TT	Dual-TT + MGTP
minADE ₂₀	6.983	3.310	2.337	<u>1.837</u>	0.966
minFDE ₂₀	12.11	5.097	4.249	<u>3.337</u>	2.107

In this experiment, models are trained on a source scene (NBA Dataset) and applied directly to a target scene (Soccer Dataset) without any form of online or offline adaptation. We compare the Dual-TT and Dual-TT+MGTP frameworks against several models known for their strong performance on the NBA dataset. As detailed in Table 5, our methods achieve the best results. Notably, the MGTP significantly boosts the generalization ability of the Dual-TT backbone, yielding improvements of 47.41% in minADE₂₀ and 36.85% in minFDE₂₀. GroupNet, with its hypergraph structure, outperforms all baselines in the NBA dataset as detailed in Table 3 of the main body. However, it exhibits limited transferability across different datasets due to its reliance on dataset-specific hyperparameter tuning. PECNet, which predicts trajectories through endpoint estimation, also shows subpar performance. Meanwhile, STAR, another model considering temporal-spatial factors, performs even worse than Dual-TT. In contrast, our Dual-TT demonstrates superior adaptability across diverse datasets, not dependent on highly specialized hyperparameters. Consequently, MGTP demonstrates robust generalization capabilities in this context due to its reduced dependency on the dataset’s domain.

B.5. Parameter Sensitivity

Within the SPT framework, we investigate the impact of two pivotal parameters on model performance: the number of serial inner updates J and parallel outer optimizations C . As shown in Fig. 7a, our results support the theory that a varied set of serial tasks improves the model’s ability to adapt to new situations, but only to a certain extent. Preceding tasks are crucial for an excellent start to learning while adding

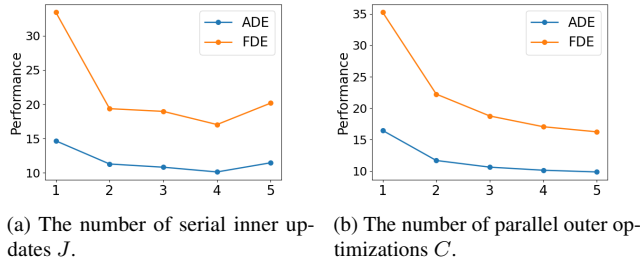


Figure 7. The impact of parameters J and C in SPT.

more tasks later has limited impact. Fig. 7b demonstrates that utilizing four parallel outer optimizations results in stable and effective outcomes. However, increasing the number of parallel optimizations beyond this threshold yields marginal benefits while incurring higher computational costs.

B.6. More Qualitative Results

As illustrated in Fig. 8, we showcase the visually optimal prediction outcomes from several models within a diverse set of unseen test scenarios from the SDD dataset. Our model’s results are most proximate to the ground truth, exhibiting the smallest distances at corresponding points. In Fig. 8 (a), within the “Coupa” scenario, the Agent-Former deviates from the ground truth. In Fig. 8 (b)(c)(d), models such as PecNet, GroupNet, and Agent-Former fail to accurately predict the agent’s trajectory along the road, instead veering off the designated path. This could imply that in scenarios involving turns, circumnavigating obstacles, or navigating complex environments, the predictive performance of these models falls short compared to our model.



Figure 8. Qualitative comparative analysis of different methods on SDD.